An Elastic-Plastic Stress Analysis in Silicon Carbide Fiber Reinforced Magnesium Metal Matrix Composite Beam Having Rectangular Cross Section Under Transverse Loading

Fuat OKUMUŞ*

1 nci Mknz. P. Tum. K. lgı, Mamak, Ankara, Turkey

In this work, an elastic-plastic stress analysis has been conducted for silicon carbide fiber reinforced magnesium metal matrix composite beam. The composite beam has a rectangular cross section. The beam is cantilevered and is loaded by a single force at its free end. In solution, the composite beam is assumed perfectly plastic to simplify the investigation. An analytical solution is presented for the elastic-plastic regions. In order to verify the analytic solution results were compared with the finite element method. An rectangular element with nine nodes has been choosen. Composite plate is meshed into 48 elements and 228 nodes with simply supported and in-plane loading condations. Predictions of the stress distributions of the beam using finite elements were overall in good agreement with analytic values. Stress distributions of the composite beam are calculated with respect to its fiber orientation. Orientation angles of the fiber are chosen as 0° , 30°, 45°, 60° and 90°. The plastic zone expands more at the upper side of the composite beam than at the lower side for 30°, 45° and 60° orientation angles. Residual stress components of σ_x and τ_{xy} are also found in the section of the composite beam.

Key Words : Composite Beam, Elasto-Plastic Analysis, Orientation Angle, Stress Analysis

1. Introduction

Metal matrix composite materials reinforced with ceramic fibers are attractive because of their high specific stiffness and strength. Advantage can be taken from the high temperature strength of ceramic fibers and the ductility of the metal matrix to produce a composite with superior combined properties. Compared to the conventional materials, the fiber reinforced composite materials presents such distinguished features as high stiffness-to- weight ratio, strength-to- weight ratio and the possibility of changing its stiffness characteristics with keeping its weight constant. Nowadays they are widely used as a primary material in various industrial areas, especially in space and military applications. They offer an increased service temperature and improved specific mechanical properties over existing metal alloys.

Elastic-plastic and residual stresses are very important in failure analysis of metal matrix composite materials. When the yield strength of the composite laminate is exceeded, the residual stresses occur in the laminated plates. The obtained residual stresses can be used to raise the yield strength of the laminated plates. Jeronimidis and Parkyn (1998) investigated residual stresses in carbon-fibre/thermoplastic matrix laminates. Bahaei-El-Din and Dvorak (1982) have investigated the elastic-plastic behavior of symmetric metal-matrix composite laminates for the case of in-plane mechanical loading. Karakuzu (1997) have given an exact solution to the elasto-plastic sress analysis of an aluminum metal-matrix composite beam reinforced by steel fibers. Residual stresses are determined in metal matrix rotating

* **E-mail** : fokumus1953@hotmail.com
TEL : +90-312-368-9525; **FAX** : +90-312-368-8690
Cigiltepe Loj. Kutan apt. No : 20 Siteler, Ankara, Turkey. (Manuscript **Received** April 21, 2003; **Revised** December 16, 2003)

discs with holes and flat plates containing notches by using finite element method and Tsai-Hill Criterion is used as the failure criterion (Karakuzu and Sayman, 1994; Karakuzu et al., 1997). An elastic-plastic stress analysis in the steel fibrous aluminum-matrix composites has been made by using the finite element method and the residual stresses have also been found (Canumalla et al., 1995; Chou et al.,1985; Sayman, 1998). Kang, G. and Kang, S.(1994) investigated the short fiber reinforced aluminum composite materials, produced by stirring method and extruded at high temperatures at different extrusion ratios.

In this paper, an elastic-plastic stress analysis in silicon carbide fiber reinforced magnesium metal matrix composite beam loaded by a single force is carried out analytically. The results have compared by finite element analysis. The composite beam whose cross section is rectangular shaped and it is cantilevered. The composite beam is assumed perfectly plastic to simplify the solution. The closed form solution of the problem is presented both in elastic-plastic regions. Tsai-Hill criterion is used as the yield criterion. The residual stress component in the beam are found by releasing the external force. During the elastic and elastic-plastic solution of the problem the external force is considered as a constant.

2. Mathematical Formulation of Elastic Solution

The mathematical expression of elastic solution of an orthotropic cantilever loaded at its free end by a single force is given by Lekhnitskii (1968). In the present study, the elastic-plastic stress analysis of a silicon carbide fibrous magnesium matrix composite cantilever beam is carried out an analytical solution to the problem is obtained. Cantilever beam of rectangular cross section is illustrated in Fig. 1. The differential equation of a plane stress case is presented by Lekhnitskii (1981) as follows,

$$a_{22}\frac{\partial^4 F}{\partial x^4}-2a_{26}\frac{\partial^4 F}{\partial x^3\partial y}+(2a_{12}+a_{66})\frac{\partial^4 F}{\partial x^4\partial y^2}-2a_{16}\frac{\partial^4 F}{\partial x\partial y^3}+a_{11}\frac{\partial^4 F}{\partial y^4}=0 \quad (1)$$

Where F is a stress function. According to Hook's law, the two-dimensional stress-strain relation in plane stress case can be written as,

$$\begin{Vmatrix}\varepsilon_x\\ \varepsilon_y\\ \gamma_{xy}\end{Vmatrix}=\begin{vmatrix}a_{11} & a_{12} & a_{16}\\ a_{21} & a_{22} & a_{26}\\ a_{16} & a_{26} & a_{66}\end{vmatrix}\begin{Vmatrix}\sigma_x\\ \sigma_y\\ \tau_{xy}\end{Vmatrix} \quad (2)$$

According to Jones (1975), in the above equation the matrix a_{ij} is the component of the compliance matrix. The compliance matrix elements are defined as follows,

$$\begin{aligned}
a_{11}&=S_{11}m^4+(2S_{12}+S_{66})m^2n^2+S_{22}n^4\\
a_{12}&=S_{12}(m^4+n^4)+(S_{11}+S_{22}-S_{66})m^2n^2\\
a_{22}&=S_{11}n^4+(2S_{12}+S_{66})m^2n^2+S_{22}m^4\\
a_{16}&=(2S_{11}-2S_{12}-S_{66})n^3m-(2S_{22}-2S_{12}-S_{66})nm^3\\
a_{26}&=(2S_{11}-2S_{12}-S_{66})n^3m-2(S_{22}-2S_{12}-S_{66})nm^3\\
a_{66}&=2(2S_{11}+2S_{22}-4S_{12}-S_{66})m^2n^2+S_{66}(m^4+n^4)
\end{aligned} \quad (3)$$

where m and n are cosine and sine of the angle θ that the loading axis x makes with the principal material (fiber) direction 1.

In Eq. (3), "S" terms are defined by the following:

$$S_{11}=1/E_1,\ S_{12}=1/E_2,\ S_{12}=-\nu_{12}/E_1,\ S_{66}=1/G_{12} \quad (4)$$

Where E_1 and E_2 are the composite's moduli of elasticity along the fiber and transverse directions, respectively.

G_{12} is the shear modulus and ν_{12} is the Poison's ratio. The stress function F is chosen as a polynomial to satisfy both the governing differential equation and the boundary condition;

$$F=\frac{d}{6}xy^3+\frac{e}{12}y^4+\frac{a}{2}y^2+bxy \quad (5)$$

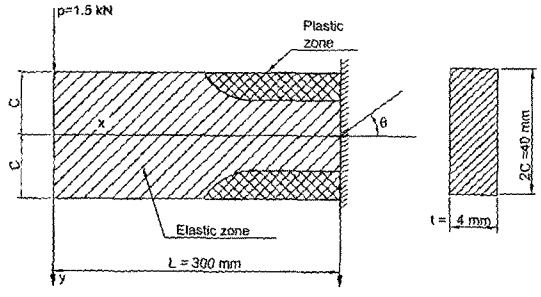

Fig. 1 Description of the problem

Substituting Eq. (5) in to Eq. (1), gives

$$-2a_{16}d+2a_{11}e=0$$
$$e=\frac{a_{16}}{a_{11}}d=sd \tag{6}$$

where $s=\frac{a_{16}}{a_{11}}$ from above equations, stress components can be witten as,

$$\sigma_x=\frac{\partial^2 F}{\partial y^2}=dxy+ey^2+a=dxy+sdy^2+a$$
$$\sigma_y=\frac{\partial^2 F}{\partial x^2}=0 \tag{7}$$
$$\tau_{xy}=-\frac{\partial^2 F}{\partial x\partial y}=-\frac{d}{2}y^2-b$$

The boundary conditions for the cantilevered beam are as follows,

$$\sigma_y=0 \text{ at } y=\pm c$$
$$\tau_{xy}=0 \text{ at } y=\pm c$$
$$\int_{-c}^{+c}\tau_{xy}\,t\,dy=-p \text{ at the free end,} \tag{8}$$
$$\int\sigma_x\,t\,dy=0 \text{ at the free end,}$$
$$\int\sigma_x\,t\,dy=0 \text{ at the free end,}$$

where t is the thickness of the beam.

By solving the above equations, the parameters a, b, d are obtained and stress components become,

$$\sigma_x=-\frac{P}{I}\left(xy+sy^2-\frac{1}{3}sc^2\right)$$
$$\sigma_y=0 \tag{9}$$
$$\tau_{xy}=-\frac{P}{2I}(c^2-y^2)$$

here I is the inertia moment of the cross-section of the beam, and is given by

$$I=\frac{2}{3}tc^3$$

Thus, both the governing differential equation and all the boundary conditions are satisfied.

3. Mathematical Formulation of Elastic-Plastic Solution

In this section, solution to the problem, is discussed where the beam material is assumed to be perfectly plastic. Strain-hardening is neglected for the simplicity of the investigation. Because the analytical solution of the composite beam is almost impossible under the condition of work-hardening. In the plastic zone, the equations of equilibrium for the plane stress case are given as follows :

$$\frac{\partial\sigma_x}{\partial x}+\frac{\partial\tau_{xy}}{\partial y}=0$$
$$\frac{\partial\tau_{xy}}{\partial x}+\frac{\partial\sigma_y}{\partial y}=0 \tag{10}$$

As mentioned earlier, the Tsai-Hill theory is used as a yield criterion in the solution. Since the composite beam possesses nearly the same yield strength in tension and compression due to reinforcing by the magnesium metal wires. Thus,

$$\sigma_1^2-\sigma_1\sigma_2+\frac{X^2}{Y^2}\sigma_2^2+\frac{X^2}{S^2}\tau_{12}^2=X^2 \tag{11}$$

where X and Y are the yield strengths of the composite beam in the principal material directions, respectively. S is the yield strength for pure shear. The stress components in the principal material directions can be written as follows,

$$\sigma_1=\sigma_x m^2+2\tau_{xy}mn$$
$$\sigma_2=\sigma_x n^2-2\tau_{xy}mn \tag{12}$$
$$\tau_{12}=-\sigma_x mn+\tau_{xy}(m^2-n^2)$$

By putting $\sigma_y=0$ in the second differential equations of equilibrium gives that τ_{xy} is a function of y in the ordinary form. Differentiating the eq. (11) with respect to x and putting $\frac{\partial\tau_{xy}}{\partial y}=0$ and then $\frac{\partial\sigma_x}{\partial x}$ is found to be zero. By substituting it in the first differential equation of equilibrium, gives that τ_{xy} is a constant. From the eq. (11), it is obtained that σ_x is a constant. Plastic zone begins at the upper and lower surfaces of the beam and σ_x on those surfaces is equal to the yield strength of the beam, therefore τ_{xy} as a constant is equal to zero. The yield point of the beam can be obtained as,

$$X_1=\left(m^4-m^2n^2+\frac{X^2}{Y^2}n^4+\frac{X^2}{S^2}m^2n^2\right)^{-1/2}X \tag{13}$$

When the plastic zone expands along the beam, σ_x becomes X_1 and τ_{xy} equals 0. From this condi-

tion, $\sigma_x=X_1$ is found as a constant in the plastic region and the shear stress is equal to zero. The plastic zone starts first at the upper surface of the beam for 30° orientation angle. But it starts on the upper and lower surfaces at the same distances fom the free end for 0 and 45° orientation angles because of symmetry of the material properties with respect to the x-axis.

When the plastic region expands both at the upper and lower surfaces, as given in Fig. 2, boundary conditions for elastic region at any section **x** are written as,

$$\tau_{xy}=0 \text{ at } y=-h_1$$
$$\tau_{xy}=0 \text{ at } y=h_2$$

At any section x resultant of τ_{xy} along the elastic region is equal to $-p$

$$\begin{aligned} &\int_{-h_1}^{h_2}\tau_{xy}\,t\,dy=-p \\ &\sigma_x=X_1 \text{ at } y=-h_1 \\ &\sigma_x=X_1 \text{ at } y=h_2 \end{aligned} \tag{14}$$

The resultant of σ_x at this section is equal to zero, Thus ;

$$X_1(c-h_1)t-X_1(c-h_2)t+\int_{-h_1}^{h_2}\sigma_x\,t\,dy=0 \tag{15}$$

and at the same time, the moment in this section can be written as follows,

$$X_1(c-h_1)\frac{c+h_1}{2}t+\frac{1}{2}X_1(c-h_2)^2t-\int_{-h_1}^{h_1}\sigma_x\,t\,dy=px \tag{16}$$

For satisfying both differential Eq. (1) and Eq. (7), the stress function in the elastic region is chosen as below,

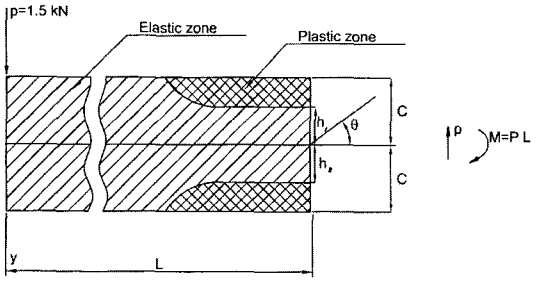

Fig. 2 Expansion of plastic zone along the beam at any section x

$$F=\frac{d}{6}xy^3+\frac{1}{12}ey^4+\frac{1}{2}ay^2+bxy+\frac{1}{2}kxy^2+\frac{1}{6}ry^3 \tag{17}$$

By using Eq. (17), the stress components are found as,

$$\begin{aligned} &\sigma_x=dxy+sdy^2+ry+kx+a \\ &\sigma y=0 \\ &\tau_{xy}=-\frac{1}{2}dy^2-ky-b \end{aligned} \tag{18}$$

From the boundary conditions, the unknown seven parameters are obtained as follows,

$$\begin{aligned} &d=-\frac{12}{t}p(h_1+h_2)^{-3} \\ &b=-\frac{1}{2}dh_1h_2 \\ &k=\frac{1}{2}d(h_1-h_2) \\ &r=[sd(h_1^2-h_2^2)-dx(h_1+h_2)-2X_1](h_1+h_2)^{-1} \\ &a=-sdh_1-\frac{X_1(h_1-h_2)}{h_1+h_2}-\frac{d(h_1-h_2)}{2}x \\ &h_1=3\left[\frac{pS}{3t}+\left(\frac{p^2S^2}{3t^2}+\frac{c^2X_1^2}{3}-\frac{c^2X_1^2}{3t}\right)^{1/2}\right]X_1^{-1} \\ &h_2=h_1-\frac{2ps}{X_1t} \end{aligned} \tag{19}$$

Determining h_1 gives all the other unknow constants and the stress components are found in order to obtain the expension of the plastic region and the residual stress components here h_1 and h_2 give the boundary of the plastic region with the respect to the x axis.

4. Finite Element Analysis

In this work, finite element procedure is employed to calculate the residual stresses and yield strength of the composite laminates. Nine-node elements are used with displacement functions. The stiffness matrix of the composite plate can be obtained by using the minimum potential energy principle. Bending and shear stiffness matrices are,

$$|K_b|=\int_A |B_b|^T|D_b||B_b|\,dA$$
$$|K_s|=\int_A |B_s|^T|D_s||B_s|\,dA$$

Where

$$|D_b| = \begin{vmatrix} A_{ij} & B_{ij} \\ B_{ij} & D_{ij} \end{vmatrix}$$

$$|D_s| = \begin{vmatrix} k_1^2 A_{44} & 0 \\ 0 & k_2^2 A_{55} \end{vmatrix} \quad (20)$$

$$(A_{ij}, B_{ij}, D_{ij}) = \int_{-h/2}^{h/2} Q_{ij}(1, z, z^2)\,dz, \quad (i, j = 1, 2, 6)$$

$$(A_{44}, A_{55}) = \int_{-h/2}^{h/2} (Q_{44}, Q_{55})\,dz$$

Here, D_b and D_s are the bending and shear parts of the material matrix, respectively. The term A_{45} has been neglected. Because, A_{45} is negligible in comparison with A_{44} and A_{55}. The shear correction factors are given by,

$$k_1^2 = k_2^2 = 5/6[12]$$

In this analysis, the external forces are applied transversely. Since, the calculated stresses do not coincide with the true stresses in a nonlinear problem, the unbalanced nodal forces and the equivalent nodal forces must be calculated. The equivalent nodal point forces corresponding to the element stresses at each iteration can be calculated as follows,

$$\{R\}_{eq.} = \int_{Vol.} |B|^T \sigma \, dA = \int_{Vol.} |B_b|^T \sigma_b \, dA + \int_{Vol.} |B_s|^T \sigma_s \, dA \quad (21)$$

When the equivalent nodal forces are known, the unbalanced nodal forces can be found by,

$$\{R\}_{unbalanced} = \{R\}_{applied} - \{R\}_{equivalent} \quad (22)$$

These unbalanced nodal forces are applied for obtaining increments in the solution and must satisfy the convergence tolerance in a nonlinear analysis. Residual stresses are very important in failure analysis of metal matrix laminated plates. When the yield point of the laminate is exceeded, the residual stresses occur in laminate plates. The obtained residual stresses can be used to raise the yield strength of the composite plates.

In this solution, 228 nodes and 48 nine-node plate elements are used. The boundary conditions for cantilever beam are shown in Fig. 3. Displacements in the x-direction were prohibited for all nodes on the rigth side of the beam. In order to obtained more accurate results at the composite plate, a highly refined mesh was constructed for all region as shown in Fig. 4.

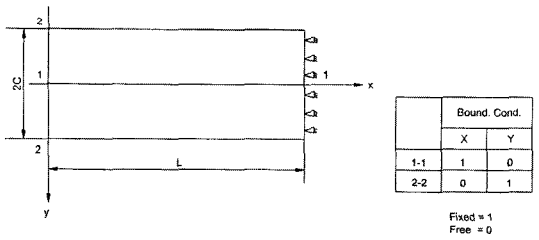

Fig. 3 Boundary condition for the finite element analysis

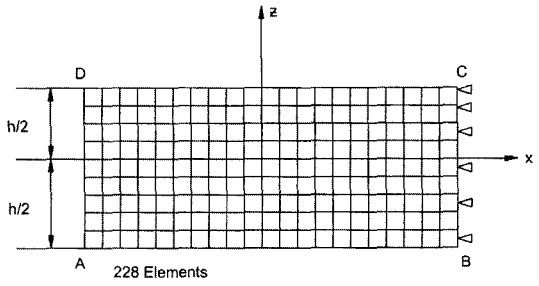

Fig. 4 Aypical finite element model of rectangular beam

5. Preparation of the Beam

In this study, silicon carbide and magnesium were used to fabricate the composite beam. The beam is constructed of the magnesium matrix and silicon carbide fibers by using moulds. The moulds are insulated and heated by electrical

Table 1 Mechanical properties of the composite material

E_1 (GPa)	E_2 (GPa)	G_{12} (GPa)	ν_{12}	Axial Strenght X (MPa)	Transverse strenght Y (MPa)	Shear strenght S (MPa)
94	82	51	0.3	245.0	28.0	59. 8

resistance up to 600℃. The silicon carbide fibers are placed between the magnesium sheets under pressure at 30 MPa. The hydraulic press has been used to apply a pressure of 30 MPa to the mould. By using manufacturing set, the yield strength of magnesium is exceeded and good bonding between matrix and fiber has been achieved. The mechanical properties and yield strengths of the composite beam are given in Table 1 are measured by using the Instron testing machine and strain gauges.

6. Numerical Results and Discussions

The cantilevered composite beam is loaded by 15 N constant single force at its free end. The thickness of the composite beam is 4 mm. The beam has 300 mm length and 40 mm height. Elastic-plastic stress analysis is carried out analytically and than the results are controlled by the finite element method. Yielding starts first at the upper and lower surfaces. When the external force is released the residual stress components are obtained. The distance between the free end and first yield strength at the upper and lower surfaces are presented in Table 2. It is shown from this table that the yielding begins earlier at the upper surfaces, for each case. When the orientation angle θ is increased the yield strength of the composite beam approaches the surface of the beam.

The expansion of the plastic zone of σ_x at the upper and lower surfaces are given in Table 3. As can be clearly seen from Table 3, when the distance from the free end is increased the plastic region becomes larger and also the intensity of the residual stress component of σ_x the upper surface becomes greater. The residual stress component of σ_x at the upper and lower surfaces of the beam are also given in Table 3 for x=65 mm to x=85 mm. The residual stress component of σ_x is represented along the cross-section of the cantilever composite beam at some sections. As shown from this Table, the intensity of σ_x is maximum both at the upper and lower surfaces of the beam. In this Table, the residual stress component of τ_{xy} in the elastic-plastic-region is given for only one section.

The expansion of the plastic zone and distribution of σ_x in case of the 0°, 30°, 45°, 60° and 90° orientation angles are given in Table 4. It is

Table 2 The distance between the free end plastic zones at the upper and lower surfaces for various orientation angles

Orientation angle (θ)	00	30°	45°	60°	90°
Distance at the upper surface (mm)	191.00	58.94	36.47	26.19	21.35
Distance at the lower surface (mm)	191.00	60.55	38.54	27.75	21.35

Table 3 The expension of the plastic zone and the residual stress component of σ_x at the upper and lower surface of the beam

x (mm)	h_1 (mm)	h_2 (mm)	$(\sigma_x)_p$ (MPa)		$(\sigma_x)_e$ (MPa)		$(\sigma_x)_r$ (MPa)	
			At the upper surface	At the lower surface	At the upper surface	At the lower surface	At the upper surface	At the lower surface
65	17.65	18.54	75.64	−75.64	81.18	−78.67	−5.54	3.03
70	15.40	16.15	75.64	−75.64	87.49	−84.45	−11.85	8.81
75	13.53	14.80	75.64	−75.64	92.17	−91.63	−16.53	15.99
80	11.18	11.76	75.64	−75.64	97.46	−97.41	−21.82	21.77
85	8.65	9.15	75.64	−75.64	102.50	−101.58	−26.86	25.94

clearly seen that, h_1 and h_2 are the same for the 0° orientation angle, and h_1 is smaller than h_2 for the beams with 30° and 45° orientation angles. It should also be noted that for all cases, the intensity of the residual stress component of σ_x is maximum at the upper and lower surfaces of the beam.

The residual stress in a beam of $\theta=0°$ orientation angle are given along the cross section, as seen in Fig. 3. The residual stress component of σ_x is represented along the cross-section of the beam at some sections. As seen from this figure, the intensity of the residual stress of σ_x is maximum and has the same value at the upper and lower surface of the beam. The shear stress component for elastic and elastic-plastic cases is given only for the cross-section at the fixed end, where x= 209 mm. The intensity of the residual stress component of the shear stress is illustrated in the same Figure. to each fiber orientation. Results have shown that the residual stress component of the shear stress is maximum where y=0.

The residual stresses for the $\theta=30°$ orientation angle is presented in Fig. 4. As seen from this Figure, the intensity of the residual stress component of σ_x is maximum at the upper and lower surfaces. It is also seen that, the plastic zone expands more at the upper side than the lower side. The intensity of the residual stress component of σ_x at the upper surface is greater than that at the lower surface. The elastic-plastic and elastic stress distribution of τ_{xy} are given at the cross-section, where x=84.45 mm.

Residual stress component of σ_x in case of 45°, 60° and 90° orientation angles is presented in cross-section in the beam as seen in Fig. 5, 6 and 7. As seen from all the Fig., when the orientation angle θ is increased the yield point of the composite beam becomes smaller, thus the plastic zone expands more rapidly. The plastic regions spreads at the upper side more than that at the lower side for the orientation angles of 30°, 45° and 60°. It is also shown that the expansion of the plastic zone for 0° and 90° is the same at the upper and

Table 4 The expansion of the plastic zone and residual stress component of σ_x at the upper and lower surface for 0°, 30°, 45° , 60° and 90° orientation angle

Orientation angle (θ)	x (mm)	h_1 (mm)	h_2 (mm)	$(\sigma_x)_p$ (MPa)		$(\sigma_x)_e$ (MPa)		$(\sigma_x)_r$ (MPa)	
				At the upper surface	At the lower surface	At the upper surface	At the lower surface	At the upper surface	At the lower surface
0°	190	18.54	18.54	238.1	−238.1	239.27	−239.27	−1.12	1.12
	195	18.31	18.31	238.1	−238.1	245.10	−245.10	−6.95	6.95
	200	17.65	17.65	238.1	−238.1	251.25	−251.25	−13.10	13.10
30°	45	14.80	16.75	48.05	−48.05	56.14	53.80	−8.09	5.75
	50	11.35	13.40	48.05	−48.05	62.18	60.14	−14.13	12.09
	55	6.11	7.85	48.05	−48.05	68.75	66.40	−20.70	18.35
45°	29.51	19.85	19.84	35.17	−35.17	43.14	−43.14	−7.97	7.97
	32.13	16.55	17.19	35.17	−35.17	46.75	−46.75	−11.58	11.58
	34.46	13.45	14.51	35.17	−35.17	49.17	−49.17	−14.00	14.00
60°	119.4	16.40	18.50	28.65	−28.65	43.10	−43.10	−0.85	0.85
	125.3	13.67	17.61	28.44	−28.44	42.15	−42.15	−1.76	1.61
	136.5	9.71	16.68	26.17	−28.17	42.20	−42.20	−2.45	2.58
90°	115.4	12.50	12.50	24.15	−24.15	36.15	−36.15	−1.51	1.60
	123.6	11.80	11.80	24.15	−24.15	36.20	−36.20	−3.45	1.45
	148.9	10.47	10.47	24.15	−24.15	36.45	−36.45	−3.91.	2.35

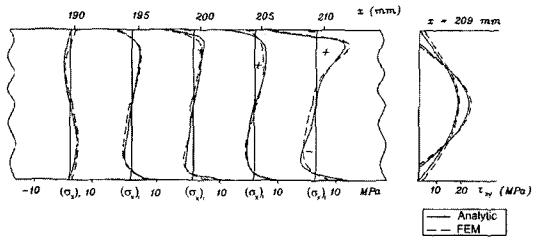

Fig. 5 Residual stresses in the beam for 0° orientation angle

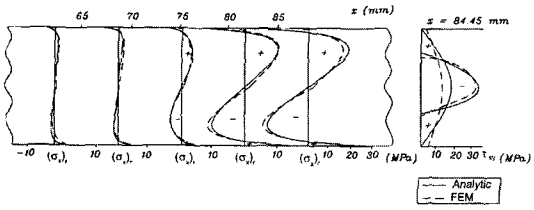

Fig. 6 Residual stresses in the beam for 30° orientation angle

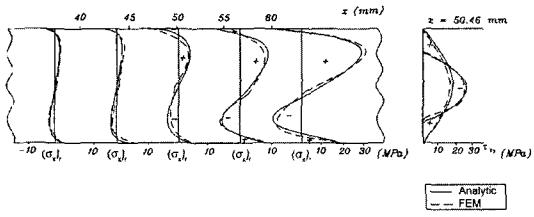

Fig. 7 Residual stresses in the beam for 45° orientation angle

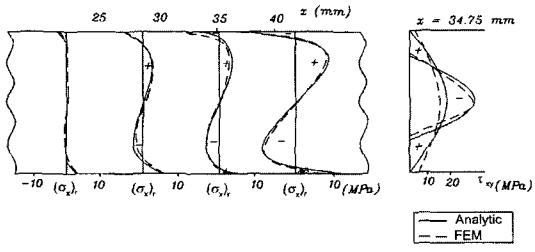

Fig. 8 Residual stresses in the beam for 60° orientation angle

lower sides of the composite beam because of the symmetry with respect to the x axes.

The expansion of the shear stress is given at the fixed end cross-section for the elastic-plastic and elastic solution. It is well known that the difference between the elastic-plastic and elastic values gives the residual stress components. The residual

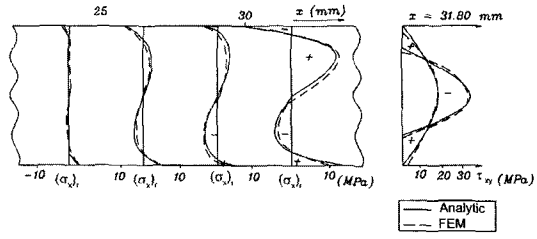

Fig. 9 Residual stresses in the beam for 90° orientation angle

stress component of the shear stress is maximum around y=0.

Concluding Remarks

In the present work, an elastic-plastic solution is obtained in a silicon carbide fibrous magnesium matrix composite beam which is loaded by a single force at its free end. Based on this study, the following remarks can be made :

(1) The expansion of the plastic zone starts first at the upper surface for 30°, 45° and 60° orientation angles.

(2) The magnitude of the residual stress component of σ_x is greatest at the upper surface of the beam.

(3) In the case of the orientation angle is increased the plastic zone expands very rapidly.

(4) The expansion of the plastic zone is symmetric for 0° and 90° orientated beams.

(5) The intensity of the residual shear stress is maximum around the y axis.

(6) The intensity of the residual stress component of σ_x is much greater than the residual stress component of τ_{xy}.

(7) The residual stresses may be use to increas the strength of the composite beam.

References

Bahei-El-Din, Y. A. and Dvorak, G. J., 1982, "Plasticity Analysis of Laminated Composite Plates," *Transactions of the ASME*, Vol. 49, pp. 740~746.

Canumalla, S., Dynan, S. A. and Green, D. J., 1995, "Mechanical Behaviour of Mullite Fiber Reinforced Aluminum Alloy Composites," *Jour-*

nal of Composite Materials, Vol. 29, pp. 653~69.

Chou, T. W., Kelly, A. and Okura, A., 1985, "Fibre-Reinforced Metal-Matrix Composites," *Journal of Composite Materials*, Vol. 16, pp. 187~206.

Jeronimidis, G. and Parkyn, A. T., 1998, "Residual Stress in Carbon Fibre-Thermoplastic Matrix Laminates," *Journal of Composite Materials*, Vol. 22, No. 5, pp. 401~15.

Jones, R. M., 1975, Mechanics of Composite Materials. Kogakuska, Tokyo : McGraw-Hill.

Kang, C. G. and Kang, S. S., 1994, "Effect of Extrusion on Fiber Orientation and Breakage of Aluminar Short Fiber Composites," *Journal of Composite Materials*, Vol. 28, pp. 155~170.

Karakuzu, R. and Sayman, O., 1994, "Elasto-Plastic Finite Element Analysis of Orthotropic Rotating Discs with Holes," *Computers and Structures*, Vol. 51, pp. 695~703.

Karakuzu, R., 1997, "Exact Solution of Elasto-Plastic Stresses in a Metal-Matrix Composite Beam of Arbitrary Orientation Subjected to Transverse Loads," *Composite Science and Technology*, Vol. 56, pp. 1383~1389.

Karakuzu, R., Ozel, A. and Sayman, O., 1997, "Elasto-Plastic Finite Element Analysis of Metal Matrix Plates with Edge Notches," *Composite Structures*, Vol. 63, pp. 551~558.

Lekhnitskii, S. G., 1968, Anisotropic Plates. Gordon and Breach Science Publishers.

Lekhnitskii, S. G., 1981, Theory of Elasticity of an Anisotropic Body. Moskow : Mir Publishers.

Sayman, O., 1998, "Elasto-Plastic Stress Analysis in Stainless Steel Fiber Reinforced Aluminum Metal Matrix Laminated Plates Loaded Transversely," *Composite Structures*, Vol. 43, pp. 147~154.